J. Membrane Biol. 141, 59–68 (1994)

The Journal of
Membrane
Biology

A Novel Cl^- Conductance in Cultured Chick Cardiac Myocytes: Role of Intracellular Ca^{2+} and cAMP

S. Liu[1], J.R. Stimers[1], M. Lieberman[2]

[1]Department of Medicine, Division of Cardiology and Department of Pharmacology, University of Arkansas for Medical Sciences, 4301 W. Markham St., MS 532, Little Rock, Arkansas 72205

[2]Department of Cell Biology, Division of Physiology, Duke University Medical Center, Durham, North Carolina 27710

Received: 18 November 1993/Revised: 16 March 1994

Abstract. Cl^- conductance in cultured embryonic chick cardiac myocytes was characterized using whole-cell patch clamp techniques. Following elimination of cation currents in Na^+- and K^+-free internal and external solutions, the basal whole-cell current was predominantly a Cl^- current. Cl^--sensitive current (I_{Cl}) was defined as the difference between the whole-cell currents recorded in normal and low $[Cl^-]_o$ when measured in the same cell. The whole-cell current in the absence or presence of 10 μM cAMP was time independent, displayed outward rectification with the pipette $[Cl^-] < 40$ mM, and was not saturated with a physiological Cl^- gradient. The Cl^- current was also activated by 1 μM forskolin and inhibited by 0.3 mM anthracene-9-carboxylic acid (9-AC). Forskolin was less effective than cAMP (internal dialysis) in activating the Cl^- current. The cAMP- or forskolin-activated and basal Cl^- current were reasonably fit by the Goldman-Hodgkin-Katz equation. The calculated P_{Cl} in the presence of cAMP was increased by five- to sixfold over the basal level. In the presence of 5 mM EGTA to decrease free $[Ca^{2+}]_i$, the whole-cell current could not be stimulated by cAMP, forskolin or IBMX (0.1 mM). These data suggest that cultured chick cardiac myocytes have a low basal Cl^- conductance, which, as in some mammalian cardiac ventricular myocytes, can be activated by cAMP. However, this study shows that the activation process requires physiological free $[Ca^{2+}]_i$.

Key words: Chloride conductance — cAMP — Calcium — Ion Channel — Cardiac Myocytes

Correspondence to: S. Liu

Introduction

Chloride currents (I_{Cl}) reported in mammalian cardiac myocytes can be divided into two groups: (1) time-independent I_{Cl} and (2) time-dependent I_{Cl}. The time-independent I_{Cl}, which is independent of intracellular Ca^{2+} (Ca^{2+}_i), can be activated by a variety of mechanisms including cAMP (Bahinski et al., 1989; Harvey & Hume, 1989; Matsuoka, Ehara & Noma, 1990), protein kinase C (Walsh, 1991), cell swelling (Sorota, 1992; Tseng, 1992) and ATP (Matsuura & Ehara, 1992). A sustained Cl^- current that is independent of cAMP and swelling has been reported by Duan, Fermini and Nattel (1992). The time-dependent I_{Cl} demonstrated by Zygmunt and Gibbons (1991, 1992) and Bouron, Potreau and Raymond (1991) was shown to be Ca^{2+} activated in rabbit atrial and ventricular myocytes (Zygmunt & Gibbons, 1991, 1992) but not in ferret ventricular myocytes (Bouron et al., 1991). At physiological levels of intracellular Cl^- concentration (~30 mM) most of these Cl^- conductances display outward-going rectification and are sensitive to 9-AC while some are sensitive to stilbene derivatives. Whether or not these I_{Cl} are carried through a single class of Cl^- channels remains unclear. Still, the modulation of Cl^- channels discussed above should depend on the activities of metabolically linked enzymes and/or the action of intracellular second messengers.

In this study, we characterize a novel Cl^- conductance in cultured embryonic chick cardiac myocytes. We show that a time-independent Cl^- conductance can be activated by cAMP-dependent pathways, and that the activation process is Ca^{2+} dependent. A preliminary report of some of these results was presented (Liu, Stimers & Lieberman, 1992).

Materials and Methods

Single Myocyte Isolation

Single cardiac myocytes were obtained from 11-day-old chick embryo hearts using a method described previously (Horres, Lieberman & Purdy, 1977) with a slight modification. Briefly, cell suspensions were obtained by disaggregating twenty 11-day-old embryonic chick hearts. Finely minced hearts were serially exposed to 0.05% trypsin in Ca^{2+}-free modified Puck's saline G solution with disaggregation being aided by gentle trituration and agitation for 4–5 cycles. Cells released during the following four exposures were collected by adding the disaggregating solution to an equal volume of ice-cold saline G containing 10% newborn calf serum to deactivate the trypsin. The resulting cell suspensions were filtered through a layer of 60 μm mesh (Nitex) and centrifuged at 800 rpm for 6 min. The supernatant was aspirated, and cells were resuspended and combined in ice-cold culture medium. Before culture, fibroblast contamination was reduced by a 45-min preferential attachment to a 100 mm culture dish. Cells were collected from suspension, centrifuged and resuspended in antibiotic-free culture medium (60% M199, 5% fetal bovine serum in a base of modified Earle's balanced salt solution). Cell counts were obtained with a hemocytometer (using trypan blue exclusion to assess cell viability), and the cells were then diluted to give a suspension of 10^7 cells/ml. Petri dishes (60 mm diameter) coated with a thin layer of agar were seeded with 0.5×10^6 cells and incubated at 37°C in 3 ml of culture medium in a 95% air + 5% CO_2 atmosphere. After 2–3 days in culture, cells were transferred for attachment to culture dishes (Falcon), which were placed on a heated inverted microscope stage (Nikon, Diaphot) for whole-cell patch clamp study.

Solutions

For all experiments, the standard extracellular control solution was a HEPES/TRIS buffered salt solution of the following composition (in mM): 145 NaCl, 5.4 KCl, 1.0 $MgCl_2$, 1.0 $CaCl_2$, 5.4 HEPES, 4.6 Tris and 5.5 glucose (pH buffered to 7.4; osmolality ~290 mOsm). Na^+- and K^+-free solutions were made by replacing $[Na^+]_o$ and $[K^+]_o$ with eqimolar tetramethylammonium chloride (TMACl). Note that the measured $[Cl^-]$ from the samples of perfusion solutions was 149.9 ± 2.3 mM (n = 29), so 150 mM was used for the control $[Cl^-]_o$ throughout the text, unless otherwise stated. External $[Cl^-]$ was varied by equimolar substitution of methanesulfonate (MSA^-). The control intracellular (pipette) solution for whole-cell patch consisted of (in mM): 150 Cs^+ (or 150 TMA^+), 4–5 Mg^{2+}, 1.0 EGTA, 0.5 Ca^{2+} (give a free Ca^{2+} of ~110 nM), 2–3 ATP, 110 Aspartate, 40 Cl^-, 5.4 HEPES, 4.6 Tris-base (pH adjusted to 7.2; osmolality ~290 mOsm). Alterations in intracellular Cl^- were made by aspartate substitution, and $MgSO_4$ was used to replace $MgCl_2$ for 1 mM Cl^- pipette solutions. Most reagents were purchased from Sigma Chemical (St Louis, MO). Cyclic AMP (Fluka), Na-8-(4-chlorophenylthio)-cAMP (cpt-cAMP, Sigma), ATP (Fluka and Sigma), anthracene-9-carboxylic acid (9-AC, Aldrich), 3-isobutyl-1-methyl-xanthine (IBMX), tetraethylammonium chloride (TEA), and 4-aminopyridine (4-AP) were directly added when needed. The stock solution (0.1 mM) of forskolin (Calbiochem) was made in dimethylsulfoxide (DMSO, Sigma), and the final concentration of DMSO (0.01%) did not alter the membrane currents. After addition of these chemicals, the pH of the solutions was readjusted.

Whole-Cell Patch Clamp

Using conventional whole-cell patch-clamp techniques (Hamill et al., 1981), single myocytes were voltage-clamped with a Dagan 9600 or an Axopatch 200 patch clamp amplifier (Axon Instruments). Heat-polished borosilicate glass (7052, Garner Glass) patch electrodes with a tip diameter of 1–2 μM were filled with the pipette solution and had a tip resistance of 1–5 MΩ. Gentle suction (~−20 cm H_2O) was used to form a gigaohm seal (3–20 GΩ) after which a brief, strong pulse of suction was applied to rupture the patched membrane to obtain the whole-cell configuration. Cells were voltage-clamped at −40 mV, and external solution was switched to Na^+- and K^+-free solution to eliminate membrane currents associated with these cations. Both capacitance and series resistance were compensated (90–95%) to reduce associated artifacts. Series resistance of 5 to 10 MΩ was measured from the amplitude of the capacity transient elicited by a 5 mV pulse before compensation or filtering. The recorded currents were low-pass filtered at 1 kHz and either stored for later analysis on videotape or directly acquired by a PC/AT computer using the Axon Labmaster DMA Acquisition System. To normalize measured currents to membrane capacitance, the capacity-transient currents recorded in response to a 5 mV hyperpolarizing pulse were integrated and divided by 5 mV to give total membrane capacitance. The average membrane capacitance of cultured single cardiomyocytes ~10 μm in diameter was 13 pF (Fig. 1), whereas small clusters of 2–3 cells had membrane capacitance that fell outside of the Gaussian distribution (≥20 pF). The variation of measured whole-cell current amplitude reported in this study is independent of the number and cell size because most of the data presented here were obtained from single cells, and the responses of small cell clusters to alteration of $[Cl^-]_o$ in the presence or absence of cAMP were not different from those of single cells, indicating good cell-cell coupling for voltage control, as well as ion and cAMP dialysis.

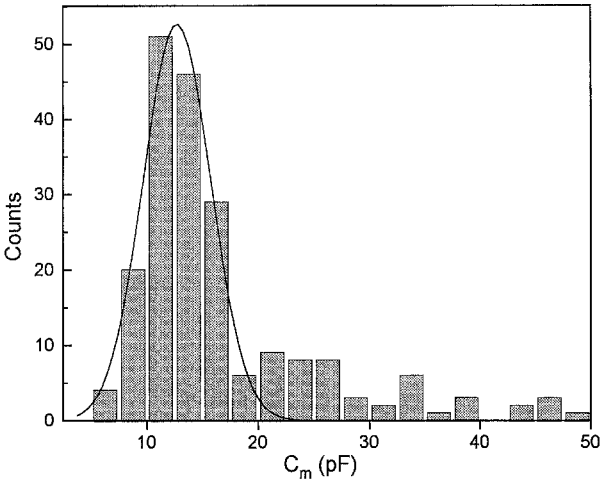

Fig. 1. Histogram of membrane capacitance (C_m) distribution for cultured heart cells. The population consisted mostly of single cells (diameter of ~10 μm) with a membrane capacitance of 12.7 ± 3.0 pF (n = 202). Cells with a C_m greater than 95% of the right tail of the Gaussian distribution (unbroken line) indicate multicellular aggregates. Bin width was 2.5 pF.

In this study, the basal current was defined as the whole-cell current remaining when membrane currents associated with Na^+ and K^+ were eliminated. Most of this current was carried by Cl^-, but other ions must also contribute (*see* Results). Two protocols were used to measure the whole-cell current. First, 300 msec voltage pulses were applied between −100 and +60 mV (or +80 mV) in 20 mV increments from a holding potential of −40 mV. The steady-state currents were measured by averaging the data points during the last 10 msec of the 300 msec pulses. Second, voltage ramps (0.2 V/sec) were ap-

plied from the holding potential of −40 to +60 mV, and subsequently from +60 to −100 mV followed by a return to −40 mV (*see inset* in Fig. 5*A*). The current measured during the hyperpolarizing segment of the ramp protocol (from +60 to −100 mV) was plotted *vs.* ramp potential to evaluate the current-voltage (*I-V*) relationship. A two-pulse protocol was used in some experiments to determine the reversal potential (a 250 msec prepulse from −40 to +10 mV followed by 300 msec test pulses between +60 and −100 mV).

To minimize liquid junction potentials, a reference electrode consisting of a 3 M KCl-agar bridge connected with a Ag/AgCl pellet was placed near the outlet of the perfusion system. By using two 3 M KCl-filled Ag-AgCl electrodes, one reference and one bath electrode, with a patch clamp amplifier (Dagan 9600), the shift in liquid junction potential on varying $[Cl^-]_o$ was minimal. All experiments were carried out at 37°C.

Analysis

Cl^--sensitive currents (I_{Cl}) were defined as the difference between currents recorded in 150 mM $[Cl^-]_o$ and low $[Cl^-]_o$. In all cases, I_{Cl} was obtained from the same cells so that each cell served as its own control. Using a Marquardt-Levenberg nonlinear least-squares curve fitting algorithm, the experimental data were best fit by the Goldman-Hodgkin-Katz (GHK) equation to obtain the Cl^- permeability (P_{Cl}).

$$I_{Cl} = P_{Cl} \cdot (V_m F^2/RT) \cdot \frac{150 - [Cl^-]_o}{(1 - \exp(-V_m F/RT))} \quad (1)$$

For some data (e.g., Fig. 6*B*), the whole-cell current was also fit by the GHK equation assuming Cl^- conductance dominates the membrane conductance in a given Cl^- gradient after elimination of most cation conductances.

$$I_{Cl} = P_{Cl} \cdot (V_m F^2/RT) \cdot \frac{[Cl^-]_o - [Cl^-]_i \cdot \exp(-V_m F/RT)}{(1 - \exp(-V_m F/RT))} \quad (2)$$

where V_m is test potential, and F, R, and T are Faraday's constant, gas constant and absolute temperature. After normalization with cell membrane capacitance, data obtained from each cell were then pooled and expressed as mean ± SEM. Paired *t*-test and one way ANOVA were used to compare the pooled data for statistical significance ($P < 0.05$).

Results

Cl^--Sensitivity of Basal Current

The basal whole-cell current was measured by eliminating membrane currents due to Na^+ and K^+. Ca^{2+} currents were not blocked; but, as shown in Fig. 2*A*, there was no indication of any time-dependent current in these experiments, suggesting that the Ca^{2+} current quickly ran down. Cells were voltage-clamped at −40 mV and internally dialyzed with Cs^+ or TMA^+ aspartate buffer containing 40 mM Cl^- and superfused with Na^+-, K^+-free solution (TMA substitute) containing 150 mM Cl^- (balanced and pH adjusted with MSA). After the membrane current stabilized (5–10 min), myocytes were perfused with various $[Cl^-]_o$ between 150 and 1 mM (MSA substitute). Figure 2*Aa* illustrates the basal current elicited by 300 msec pulses recorded from a myocyte that was internally dialyzed with a pipette solution containing 40 mM Cl^- without cAMP. Reducing $[Cl^-]_o$ caused a slight decrease in the current and a positive shift of the reversal potential (Fig. 2*Ba*), indicating that this current is at least partially mediated by Cl^-. Figure 2*Ba* illustrates the voltage and $[Cl^-]_o$ dependence of this basal current. When results from all experiments were pooled, the magnitude of this basal current at +60 mV was 3.3 ± 0.8 pA/pF ($n = 13$) with 150 mM $[Cl^-]_o$ (*see* Table 1).

cAMP-activated Cl^--sensitive Current

In contrast, when 10 μM cAMP was added to the pipette solution, there was a dramatic increase in the time-independent membrane current and this current was sensitive to the reduction of $[Cl^-]_o$ (Fig. 2*Ab*). Figure 2*Bb* illustrates the voltage dependence of the steady-state whole-cell current in the presence of cAMP. The figure shows that reduction in $[Cl^-]_o$ was associated with a decline in the outward current (inward movement of Cl^-) and a positive shift in the reversal potential. On average, the whole-cell current measured at +60 mV was 12.2 ± 3.3 pA/pF ($n = 10$) in the presence of cAMP, which was significantly different from that recorded in the absence of cAMP ($P < 0.01$, *see* Table 1). While cAMP caused a significant increase in the whole-cell current and the Cl-sensitive component of that current, a large variability occurred in the response of individual cells to cAMP stimulation, as indicated by the increase in the standard error in the presence of cAMP. In fact, 14 of 55 cells tested with cAMP exhibited a whole-cell current at +60 mV which was no larger than the mean whole-cell current without cAMP.

Reversal Potentials

While Fig. 2*Ba* clearly shows a Cl^--sensitive component of the basal whole-cell current, the shift in reversal potential of only 30–40 mV suggests that the membrane does not behave as a perfect Cl^--electrode. Changing $[Cl^-]_o$ from 150 to 9.4 mM is expected to shift the Cl^- reversal potential by +74 mV. Deviation in the shift in reversal potential from this value suggests that other ions contribute to the whole-cell current through a background conductance or leak. The reversal potentials shown in Fig. 2*Bb* are shifted by +50 mV per decade change in $[Cl^-]_o$ (>10 mM), close to the value of 61.5 mV expected from the Nernst equation for the Cl^- electrode and consistent with values reported in the literature for Cl^--sensitive currents in mammalian cardiac myocytes (Harvey & Hume, 1989; Matsuura &

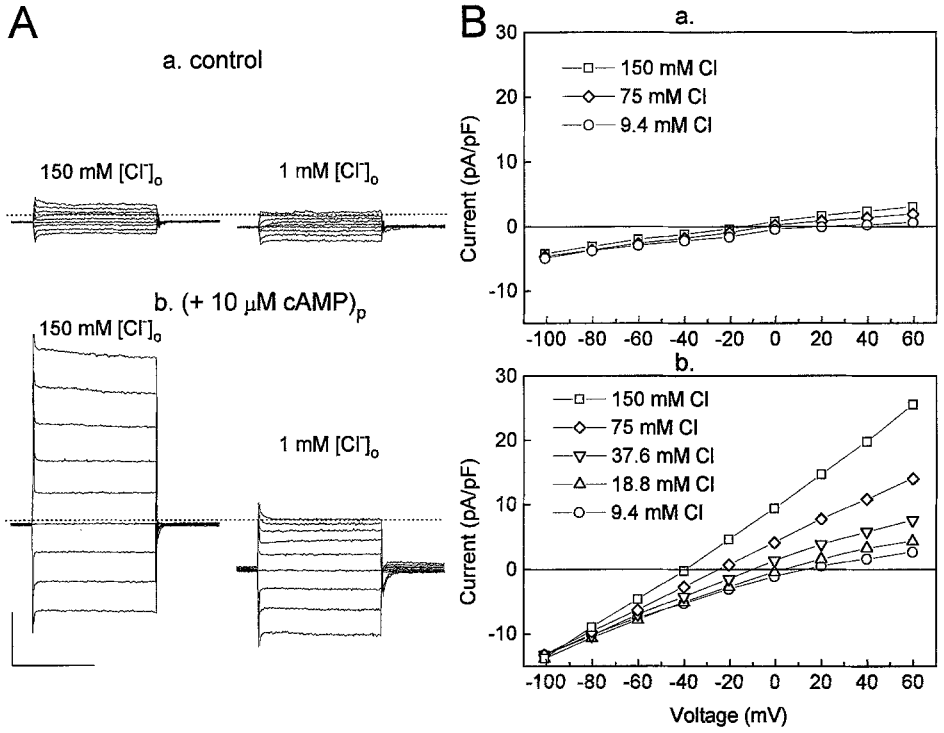

Fig. 2. cAMP activates the whole-cell Cl^- current. (*A*) Superimposed current families measured from two cells that were internally dialyzed with solutions containing 40 mM Cl in the absence (*a*) and presence (*b*) of 10 μM cAMP and externally superfused with 150 mM [Cl^-] and then 1 mM [Cl^-]. (*a*) The whole-cell current in the absence of cAMP was sensitive to the reduction of $[Cl^-]_o$, suggesting a finite basal permeability to Cl^-. (*b*) Intracellular cAMP (10 μM) induced a time-independent current that was more sensitive to changes in Cl^- gradient than the absence of cAMP. (*B*) The *I-V* relationships from data shown in *A* plus other data in the same cells. The currents were normalized by membrane capacitance. Cell membrane capacitance (C_m) was 16 pF for the cell in (*a*) and 12 pF for the cell in (*b*). Calibration: 100 pA and 200 msec for both conditions.

Ehara, 1992). The shift in reversal potential with 10 μM cAMP is closer to that expected for a Cl^- electrode and suggests that cAMP increases the membrane conductance for Cl^- relative to the background conductance; however, cAMP also increased the background conductance. As shown in Table 1, the Cl^--sensitive current was increased 4.6-fold at the same time that the Cl^--insensitive component of the whole-cell current was increased by 2.4-fold. While we have not identified the ion(s) responsible for this background current, our experimental protocols should minimize its contribution to the results. By subtracting current records obtained in the same cell in 150 mM and low $[Cl^-]_o$, we were able to investigate and describe the Cl^--sensitive current in chick cardiac myocytes.

Cl^--SENSITIVE CURRENT

The Cl^--sensitive current (I_{Cl}, *see* Material and Methods) is illustrated in Fig. 3 (symbols). I_{Cl} was reasonably fit by the GHK equation (dotted lines, *see* Materials and Methods). Assuming a specific membrane capacitance of 1 μF/cm^2, the estimated P_{Cl} ($\times 10^{-7}$ cm/sec) for cells in the absence (open symbols in Fig. 3) and presence of cAMP (filled symbols in Fig. 3) was 0.79 ± 0.02 and 6.94 ± 0.15 (averaged from 150 mM to 75, 37.6, 18.8, 9.4 and 1 mM), respectively. These results confirm that cAMP activates a Cl^- current in chick myocytes.

As illustrated in Figs. 2*A* and Fig. 4, with 1 mM $[Cl^-]_o$ the whole-cell current measured at +60 mV is virtually 0 in both basal and cAMP-stimulated myocytes. Consequently, plotting the current measured at +60 mV *vs.* $[Cl^-]_o$ shows the Cl^- dependence of I_{Cl}. Figure 4 shows that other than the demonstrated increase in magnitude there was no significant difference between the substrate dependence of the basal and cAMP-activated I_{Cl}. Curve fitting with the Hill equation showed that both basal and cAMP-activated I_{Cl} had a similar half-activation concentration ($K_{0.5}$) (126 ± 48 mM and 82 ± 8 mM for cAMP and basal Cl^- current, respectively) and Hill coefficient (1.4 ± 0.2 and 1.1 ± 0.1 for cAMP and basal Cl^- current, respectively), and neither was saturated at physiological levels of $[Cl^-]_o$. The maximum cAMP-activated I_{Cl} ($I_{Cl\text{-}max}$) was 17.1 ± 5.6 pA/pF (n = 4), which was significantly greated than the basal $I_{Cl\text{-}max}$ of 2.0 ± 0.4 pA/pF (n = 4, $P < 0.05$).

Table 1. Comparison of basal and cAMP-activated Cl^- current

Pipette solutions	I_{WC} (pA/pF)	I_{Cl} (pA/pF)	P_{Cl} ($\times 10^{-7}$ cm/sec)
40 mM Cl			
−cAMP	3.3 ± 0.8 (13)	1.9 ± 0.5 (13)	0.5 ± 0.1 (13)
+cAMP (10 μM)	12.2 ± 3.3[a] (10)	8.8 ± 3.2[a] (7)	2.6 ± 1.0[b] (7)
1 mM Cl			
−cAMP	6.1 ± 0.9 (11)	1.2 ± 0.4 (7)	0.5 ± 0.1 (7)
+cAMP (10 μM)	13.7 ± 3.1[c] (19)	13.7 ± 5.3[c] (5)	3.4 ± 1.4[c] (5)

I_{WC}: whole-cell currents. [a,b,c] $P < 0.01$, 0.02, 0.05, respectively, compared with control (−cAMP) cells. Values are means ± SE (number of cells). Current amplitudes were measured at +60 mV. Cl^- permeability (P_{Cl}) was estimated from fitting the GHK equation (Eq. 1) to the data.

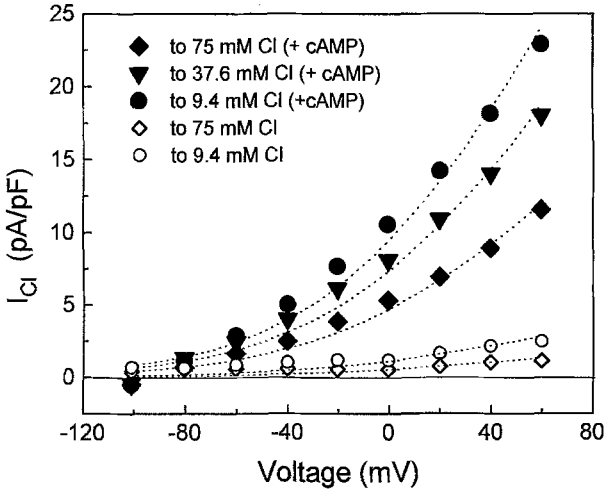

Fig. 3. Basal and cAMP-activated Cl^--sensitive currents (I_{Cl}): I_{Cl} is defined as the difference between currents measured when $[Cl^-]_o$ was changed from 150 mM to low concentrations. Both basal (open symbols) and cAMP-activated (filled symbols) I_{Cl} were reasonably fit by the GHK equation (dotted lines, *see* Materials and Methods). Averaged P_{Cl} ($\times 10^{-7}$ cm/sec) from five changes of $[Cl^-]_o$ (75, 37.6, 18.8, 9.4, 1 mM) were 0.79 ± 0.02 and 6.94 ± 0.15 for basal and cAMP-activated I_{Cl}, respectively.

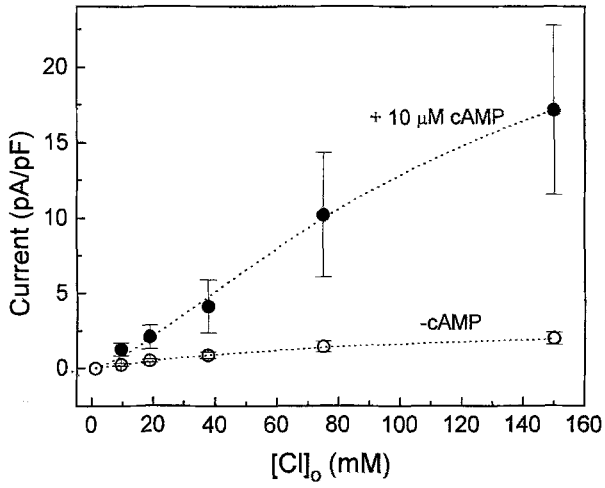

Fig. 4. Substrate dependence of Cl^- current. Cells were internally dialyzed with solutions containing 40 mM Cl^- with or without 10 μM cAMP and externally superfused with solutions containing different concentrations of $[Cl^-]_o$. The amplitudes of the whole-cell currents measured at +60 mV were plotted *vs.* corresponding $[Cl^-]_o$ in the absence (open circles) and presence of cAMP (filled circles). Dotted lines represent the best fit of the Hill equation ($I = I_{max}/(1 + (K_{0.5}/[Cl^-]^n)$. The estimated maximal current density (I_{max}) was 31 ± 8 and 3.0 ± 0.1 pA/pF for cAMP and basal whole-cell current, respectively. The half-maximal activation concentration ($K_{0.5}$) was 126 ± 48 and 82 ± 8 mM for cAMP and basal current, respectively. The Hill coefficient was 1.4 ± 0.2 and 1.1 ± 0.1 for cAMP and basal Cl^- current, respectively. Values are mean ± SEM with $n = 4$.

In other experiments, the whole-cell current was also elicited with both pulse and voltage ramp protocols (*see* Materials and Methods) to compare the results obtained with each protocol. Figure 5*A* shows the whole-cell current recorded from a cell internally dialyzed with 10 μM cAMP and 1 mM Cl^- in 150 mM $[Cl^-]_o$ solution. Membrane currents elicited with 300 msec voltage pulses (filled symbols) were identical to those elicited with the ramp protocol (unbroken lines) as well as currents measured with a two-pulse protocol (open symbols). Reduction of $[Cl]_o$ to 1 mM caused a decrease in current amplitude and slope conductance and a shift of the zero-current potential to a more positive potential, consistent with the results described in Fig. 2. Similarly, Fig. 5*B* illustrates the I_{Cl} (the difference ramp current, trace *c*) induced by the change of $[Cl^-]_o$. These data were well fit by the GHK equation (dotted line, Eq. 1) with a P_{Cl} of 8.5×10^{-7} cm/sec, similar to that obtained from the cell shown in Fig. 3*B*. The amplitude of the whole-cell current and I_{Cl} (at + 60 mV) and the P_{Cl} estimated from cells treated with and without 10 μM cAMP are summarized in Table 1. These results demonstrate that 10 μM cAMP significantly activates Cl^- conductance in cultured heart cells.

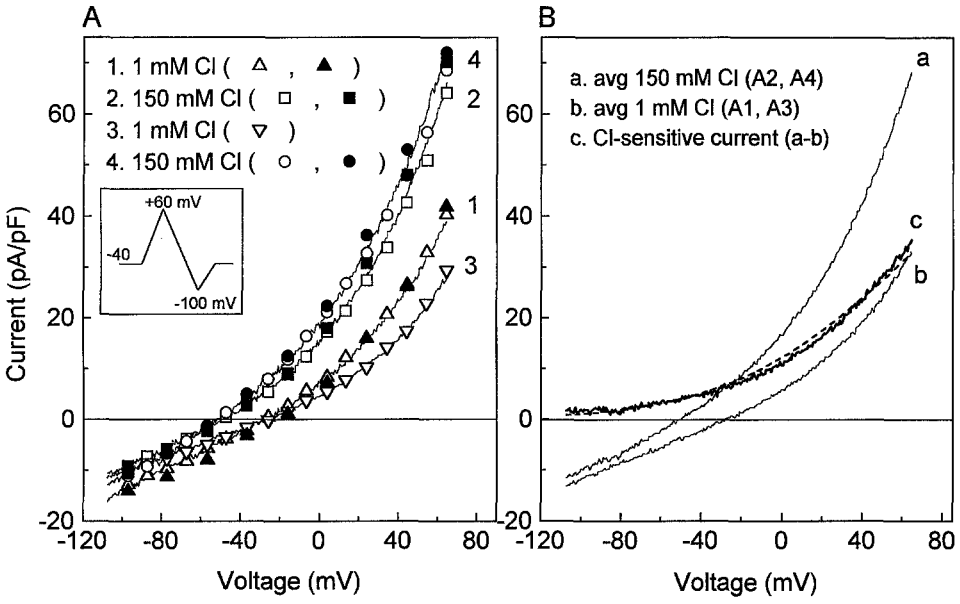

Fig. 5. Comparison of currents measured with voltage ramp and with conventional pulse protocol. (*A*) Cell was internally perfused with 1 mM Cl and 10 μM cAMP, and $[Cl^-]_o$ in bath solutions was changed in the order indicated. The cell was tested in the different solutions by applying 300 msec pulses (filled symbols), prepulse protocol (open symbols) and voltage ramp (unbroken lines). The current in the first exposure to 1 mM $[Cl^-]_o$ was greater than that in the second exposure to 1 mM $[Cl^-]_o$, possibly due to a shorter duration of exposure to 1 mM $[Cl^-]_o$ solution. The inset illustrates the ramp protocol. (*B*) Averaged currents in each solution (*a, b*) are plotted. The difference current (*c*) measured with ramp protocol was well described by the GHK equation. C_m:11 pF.

The Effect of Forskolin on I_{Cl}

To further support the activation of I_{Cl} by cAMP, whole-cell currents were examined in the presence of forskolin (FSK) which directly activates membrane bound adenylate cyclase to increase intracellular cAMP content. Cells were internally dialyzed with cAMP-free solution containing 30 mM $[Cl^-]_i$ and superfused with solutions containing 1 μM forskolin. Figure 6*A* shows that forskolin increased the whole-cell membrane current without changing the zero-current potential. The addition of forskolin more than doubled the whole-cell current (7.5 ± 1.0 pA/pF, $n = 10$; compared to control of 3.4 ± 0.3 pA/pF, $n = 27$, $P < 0.02$; *see* Table 2). Augmentation of the whole-cell current by forskolin appeared to increase with time (trace *2* measured at 3.5 min and trace *5* measured at 7.5 min in the presence of forskolin in Fig. 6*A*). A subsequent reduction of $[Cl^-]_o$ to 1 mM shifted the zero-current potential to a more positive potential and suppressed the membrane current as expected for Cl^--mediated current. Figure 6*B* illustrates the I_{Cl} induced by forskolin and the fit of the GHK equation (P_{Cl} of 1.9×10^{-7} cm/sec). If we assume that the forskolin-sensitive current is a I_{Cl} such as is found in some mammalian ventricular myocytes (Bahinski et al., 1989; Harvey & Hume, 1989), then for $[Cl^-]_i/[Cl^-]_o$ of 30 mM/145 mM (measured values) the GHK equation (Eq. 2) gives a P_{Cl} of 3.1×10^{-7} cm/sec (dashed line *2'* in Fig. 6*B*). The effect of forskolin on I_{Cl} is summarized in Table 2. Forskolin increased the amplitude of whole-cell currents by 2.2-fold, and I_{Cl} and P_{Cl} by 2.8-fold.

In addition, when cells were superfused with 0.3 mM cpt-cAMP, a membrane permeant cAMP analogue, the whole-cell current was increased by 34 ± 19% (averaged current amplitude measured at +60 mV: 5.2 ± 0.9 pA/pF [$n = 5$], compared to 4.0 ± 0.4 pA/pF of control, $n = 6$; $P > 0.05$). Nevertheless, the effect of forskolin and cpt-cAMP on the activation of I_{Cl} appears to be smaller than that of direct intracellular dialysis of cAMP (*compare* Table 2 with Table 1). One possible explanation for these results is that the concentration of cAMP resulting from forskolin and cpt-cAMP would have been diluted by the pipette solution during the whole-cell patch clamp.

The Effect of 9-AC on the cAMP-activated I_{Cl}

Anthracene-9-carboxylate (9-AC) very effectively blocks the Cl^- channel in skeletal muscle (IC_{50}, 10 μM) (Palade & Barchi, 1977) and has been shown to block both the cAMP- and swelling-activated I_{Cl} in mammalian heart cells (Harvey & Hume, 1989; Sorota, 1992; Tseng, 1992). We then tested the effectiveness of 9-AC on the cAMP-activated I_{Cl} in cultured heart cells. Cells were internally dialyzed with solutions containing 1 mM Cl^- and 10 μM cAMP. Figure 7*A* shows that 9AC (0.3 mM) applied for 2.5 min to the bath solution (150 mM $[Cl^-]_o$) inhibited the cAMP-activated I_{Cl}. The addition of 9AC (0.1 or 0.3 mM) caused the current to decrease by 43.6

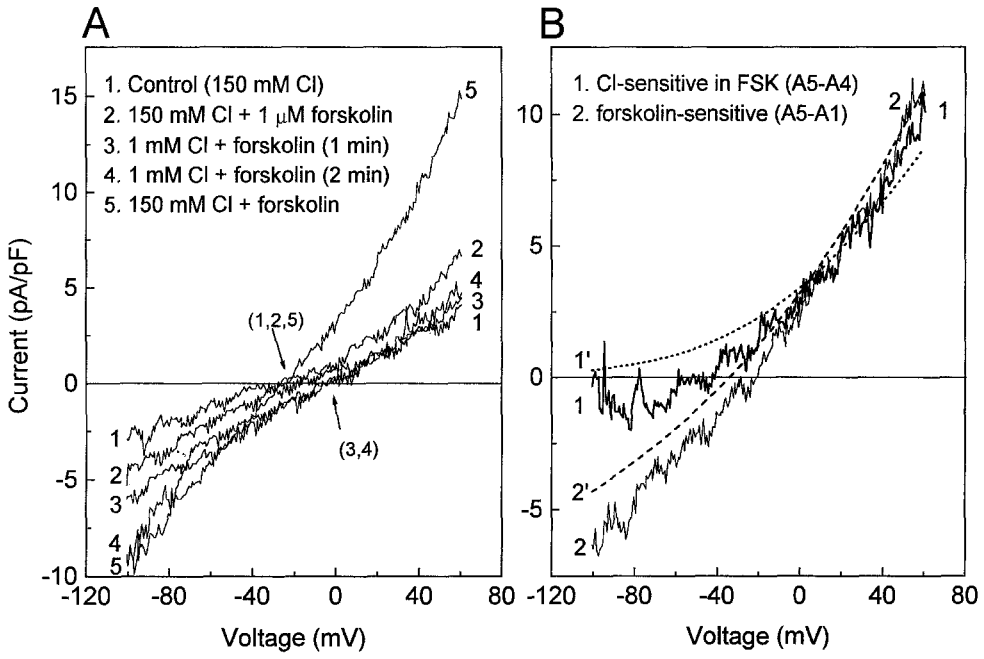

Fig. 6. Effect of forskolin on the whole-cell Cl^- current. (*A*) Cell was internally dialyzed with 30 mM [Cl^-] and superfused with control solution containing 150 mM TMACl (trace *1*). The addition of 1 μM forskolin (FSK) for 3.5 min increased the whole-cell current (trace *2*) without a shift of zero-current potential (downward arrow). Reduction of $[Cl^-]_o$ to 1 mM caused a decrease in current (trace *3*) and a shift of the zero-current potential to a more positive potential (upward arrow). In the presence of FSK and 1 mM $[Cl^-]_o$, the whole-cell current slightly increased with time in both inward and outward directions in response to hyperpolarizing and depolarizing pulses (trace *4*). Restoration of $[Cl^-]_o$ to 150 mM revealed a greater current than before (trace *5*, compared to trace *2*). (*B*) I_{Cl} (trace *1*) and the FSK-induced current (trace *2*). I_{Cl} was reasonably fit by the GHK equation with P_{Cl} of 2.4×10^{-7} cm/sec. If we assume that the forskolin-sensitive current is a Cl^- current (I_{Cl}), this current can also be fit by the GHK equation (thin dotted line (trace *2'*)) for $[Cl^-]_o/[Cl^-]_i$ of 150/30 mM. C_m: 7 pF.

Table 2. Effect of forskolin on the Cl^- current

External solutions	I_{WC} (pA/pF)	I_{Cl} (pA/pF)	P_{Cl} ($\times 10^{-7}$ cm/sec)
$(30\ mM\ Cl)_p$			
Control	3.4 ± 0.3 (27)	1.7 ± 0.4 (19)	0.5 ± 0.1 (19)
+Forskolin (1 μM)	7.5 ± 1.9[a] (10)	4.8 ± 1.8[a] (7)	1.4 ± 0.5[b] (7)
$(1\ mM\ Cl)_p$			
Control	6.1 ± 0.9 (11)		
+IBMX[c]	8.6 ± 2.3 (11)	ND	ND
+Forskolin +IBMX	15.7 ± 5.2 (5)		

I_{WC}: whole-cell currents. [a,b] $P < 0.02$ and 0.05, respectively, compared with control cells. [c] IBMX (0.1 mM) was added into pipette solutions. $(\ )_p$: Cl^- concentration in pipette solutions. ND: not determined.

± 4.5% (n = 3) when measured at +60 mV in the presence of cAMP. After washout of 9-AC and recovery of I_{Cl}, subsequent reduction of $[Cl^-]_o$ to 1 mM decreased the membrane current to the same level as did 9-AC. Figure 7*B* shows that the 9-AC-suppressed current was essentially identical to the cAMP-activated I_{Cl}.

$[Ca^{2+}]_i$ Is Required for cAMP to Activate the Cl^- Conductance

Since the cAMP-activated Cl^- conductance was measured at a free $[Ca^{2+}]_i$ of 110 nM, we questioned whether the presence of a physiological level of $[Ca^{2+}]_i$ is essential for cAMP activation. Cells were internally dialyzed with solutions containing 10 μM cAMP or 0.1 mM IBMX (an inhibitor of phosphodiesterase that increases cell cAMP), 1 mM Cl^- and 5 mM EGTA to reduce free $[Ca^{2+}]_i$ below 10 nM. Figure 8 shows that with $[Ca^{2+}]_i$ less than 10 nM, the cAMP-activated I_{Cl} was significantly reduced (compared with Figure 5*B*, trace *a*). Whole-cell currents measured at +60 mV were 4.2 ± 0.5 pA/pF (n = 16) for 10 nM free $[Ca^{2+}]_i$ but were 11.8 ± 2.1 pA/pF (n = 30) for 110 nM free $[Ca^{2+}]_i$, $P < 0.02$. There was no significant I_{Cl} (trace *3*, Fig. 8*A*) when free

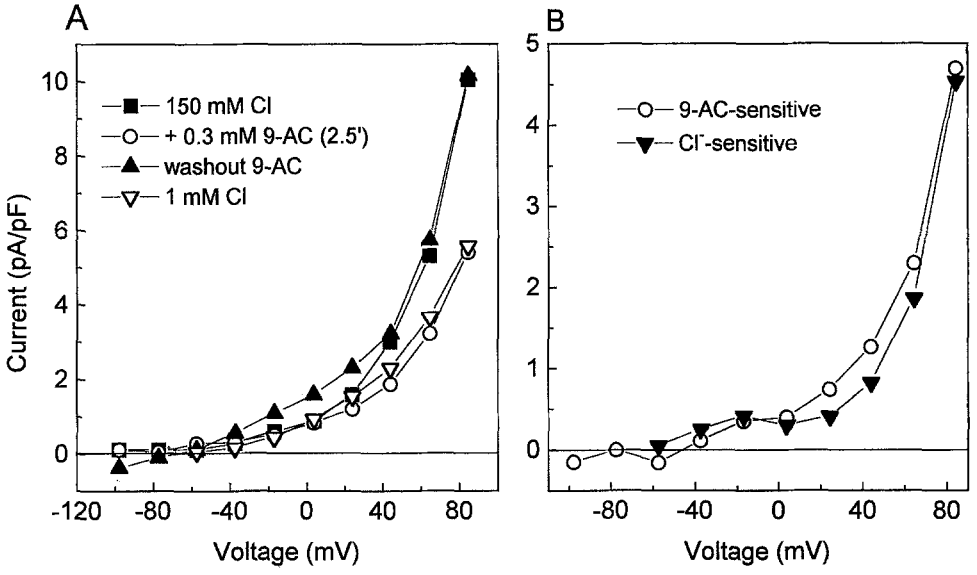

Fig. 7. Effect of 9-AC on the cAMP-activated current. (*A*) Cell was internally dialyzed with the pipette solution containing 1 mM [Cl^-] and 10 μM cAMP. The *I-V* relationship of cAMP-activated whole-cell current in 150 mM TMACl (filled squares) was reversibly suppressed by addition of 0.3 mM 9-AC (open circles). After washout of 9-AC in the control solution, reduction of $[Cl^-]_o$ to 1 mM decreased the whole-cell current to the same level as in the presence of 9-AC (open triangles). (*B*) The 9-AC-sensitive current (open circles) appears to be nearly identical to the Cl^--sensitive current (filled triangles), suggesting that 9-AC blocked the Cl^- current. C_m: 18 pF.

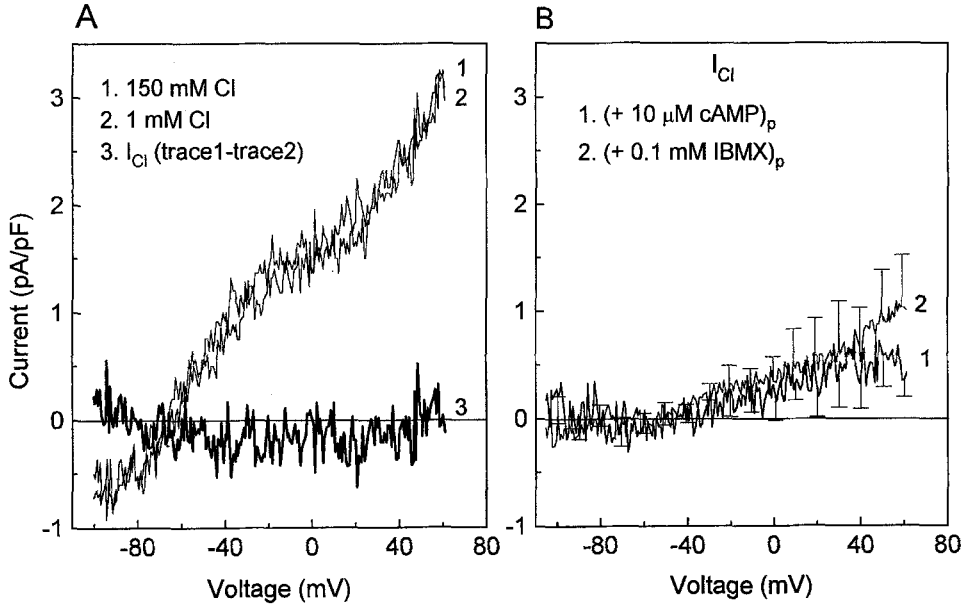

Fig. 8. Low free $[Ca^{2+}]_i$ suppresses the Cl^- current. (*A*) Cell was internally dialyzed with solution containing 1 mM [Cl^-], 10 μM cAMP and 5 mM EGTA (trace *1*). Under this condition of low free $[Ca^{2+}]_i$ (~10 nM), reduction of $[Cl^-]_o$ to 1 mM did not alter the whole-cell current in the presence of cAMP (trace *2*). C_m = 25 pF. The Cl^--sensitive current in low $[Ca^{2+}]_i$ (trace *3* in *A* and trace *1* (n = 3), in *B*) was much smaller than that in normal $[Ca^{2+}]_i$ (e.g., Fig. 5). (*B*) When cells were internally dialyzed with a similar low $[Ca^{2+}]$ pipette solution but 0.1 mM IBMX instead of cAMP, I_{Cl} was also small (n = 4).

$[Ca^{2+}]_i$ was less than 10 nM. Other experiments showed that 9-AC also had no effect on the cAMP-activated whole-cell current when free $[Ca^{2+}]_i$ was less than 10 nM (*data not shown*). The absence of I_{Cl} when $[Ca^{2+}]_i$ < 10 nM (*see* Fig. 8*A*) suggests that a decrease of $[Ca^{2+}]_i$ suppressed both basal and cAMP-activated I_{Cl}. When cells were internally dialyzed with 5 mM EGTA and 0.1 mM IBMX, I_{Cl} was also suppressed (Fig. 8*B*). The

comparison of cAMP-activated I_{Cl} in 10 and 110 nM free $[Ca^{2+}]_i$ is summarized in Table 3. Furthermore, under conditions of $[Ca^{2+}]_i < 10$ nM plus IBMX in the pipette solution, addition of 1 μM forskolin to the bath solution did not enhance the whole-cell current (an increase of $-0.2 \pm 8.3\%$ and $92.8 \pm 37.9\%$ in 10 and 110 nM free $[Ca^{2+}]_i$, respectively). These results suggest that cAMP-activated as well as basal I_{Cl} require the presence of a physiological level of free $[Ca^{2+}]_i$.

Table 3. Effect of $[Ca^{2+}]_i$ on I_{Cl}

Pipette solutions	I_{Cl} (pA/pF)	P_{Cl} ($\times 10^{-7}$ cm/sec)
1 mM Cl + 1 mM EGTA		
control	1.3 ± 0.3* (9)	0.5 ± 0.1* (9)
+cAMP	16.7 ± 5.7 (4)	4.2 ± 1.5 (4)
1 mm Cl + 5 mM EGTA		
+cAMP or IBMX	0.7 ± 0.3* (7)	0.2 ± 0.1* (7)

* $P < 0.01$, compared with cells treated with 10 μM cAMP and calculated 110 nM free $[Ca^{2+}]$. Current amplitude of I_{Cl} was measured at +60 mV. I_{Cl} and P_{Cl} in low $[Ca^{2+}]_i$ were not significantly different from the basal Cl^- current at a physiological level of free $[Ca^{2+}]$.

Discussion

The present study in cultured embryonic chick cardiac myocytes demonstrates the presence of a low basal Cl^- conductance that is activated by cAMP and requires a physiological level of free $[Ca^{2+}]_i$.

Basal Cl^- Conductance

After eliminating most of the cation currents, the basal whole-cell current is small, ~3 pA/pF (measured at +60 mV). The basal whole-cell current contains a Cl^--sensitive component that can be reasonably fit by the GHK equation with an estimated P_{Cl} of 0.5×10^{-7} cm/sec (Table 1). These results are contrary to the findings obtained from guinea-pig ventricular myocytes in which basal Cl^- conductance is negligible (Hwang, Horie & Gadsby, 1993). The discrepancy of the basal Cl^- current in these preparations may be due to the different activities of enzymes involved in the phosphorylation and dephosphorylation of the Cl^- conductance (Hwang et al., 1993). Nevertheless, the basal Cl^- conductance associated with a cardiac action potential may contribute an outward current following the upstroke (Phase 0) resulting in repolarization of the membrane potential.

Activation of Cl^- Conductance by Intracellular cAMP

In cultured cardiac myocytes, cAMP activates Cl^- conductance in a way similar to that found in mammalian ventricular myocytes (Bahinski et al., 1989; Harvey & Hume, 1989; Matsuoka et al., 1990) and in noncardiac cells expressing the cystic fibrosis transmembrane conductance regulator (Anderson et al., 1991). Forskolin also caused an increase in whole-cell current in cultured cardiac myocytes as it does in mammalian ventricular myocytes (Bahinski et al., 1989; Harvey & Hume, 1989; Matsuoka et al., 1990). The substrate dependence of cAMP-activated I_{Cl} was also reasonably described by the Hill equation and was comparable to that of basal I_{Cl} with an ~8-fold higher $I_{Cl\text{-}max}$. Neither cAMP-activated nor basal I_{Cl} were saturated under physiological conditions.

Possible mechanisms by which cAMP activates the Cl^- channel include an increase in (i) the open-state probability of Cl^- channels, (ii) the number of Cl^- channels available to open, and (iii) the unitary conductance. However, the mechanism responsible for the activation of Cl^- by cAMP cannot be distinguished in this study. Regardless, in physiological conditions, the cAMP-activated Cl^- conductance may counteract the influence of an activated Ca^{2+} channel that may occur with high sympathetic tone (Bahinski et al., 1989).

Requirement of Physiological $[Ca^{2+}]_i$ to Activate the Cl^- Conductance

Activation of Cl^- conductance by cAMP requires a physiological free $[Ca^{2+}]_i$ based on the observation that (i) decreasing pipette $[Ca^{2+}]$ in the presence of cAMP suppressed the I_{Cl} and (ii) addition of forskolin in the presence and absence of internal dialysis of IBMX in low $[Ca^{2+}]_i$ failed to activate I_{Cl}. The results of a decrease in free $[Ca^{2+}]_i$ suppressing both basal and cAMP-activated Cl^- currents suggest that physiological free $[Ca^{2+}]_i$ is required for the gating property of Cl^- channel opening, i.e., Ca^{2+}-dependent Cl^- conductance, and/or the activation of Cl^- channels by cAMP. The Ca^{2+} dependence of Cl^- conductance in these preparations is similar to that reported for rabbit cardiac myocytes (Zygmunt & Gibbons, 1991, 1992), although the latter is time dependent because of the transient Ca^{2+} current. However, in this study, the Ca^{2+} current is not observable, and the presence of Ca^{2+} channel blocker, 1 μM nifedipine, did not affect the forskolin-enhanced I_{Cl} (*unpublished data*). These results are also contrary to those obtained from guinea-pig ventricular myocytes (Bahinski et al., 1989; Harvey & Hume, 1989; Matsuoka et al., 1990). Several possibilities to explain this discrepancy are (i) the methodology used in these studies, (ii) a difference in the mechanism responsible for Cl^- channel activation, and (iii) different Cl^- channels in these preparations. Furthermore, the small size of the

spherical cultured cardiac myocytes enables rapid and complete equilibration between the pipette solution and the intracellular milieu. Because of the small cells, 5 mM EGTA should efficiently reduce free $[Ca^{2+}]_i$ to the expected value of ~10 nM and eliminate the possible contribution of Ca^{2+} release from SR. Under these conditions, the amplitude and P_{Cl} of I_{Cl} are smaller than those of basal Cl^- current (0.4 pA/pF and 1.5×10^{-8} cm/sec *vs.* 1.2 pA/pF and 5×10^{-8} cm/sec for the basal level), indicating some degree of activation of basal Cl^- conductance or existence of a Ca^{2+}-dependent portion of basal Cl^- conductance. On the other hand, if the basal Cl^- conductance in cultured heart cells reflects the basal state of protein phosphorylation of the Cl^- channel, these results would indicate that the activation process via protein kinase A is Ca^{2+} dependent. The requirement of the physiological level of free $[Ca^{2+}]_i$ to activate the cAMP-induced Cl^- conductance suggests that normal $[Ca^{2+}]_i$ is essential for the phosphorylation process of Cl^- channels and/or is counteracting the dephosphorylation of Cl^- channels. Distinguishing between these two possible mechanisms requires further study.

In summary, cultured chick cardiac myocytes possess a finite basal Cl^- conductance that is activated by cAMP but requires a physiological level of free $[Ca^{2+}]_i$.

We thank Meei-Yueh Liu, Kathleen Mitchell, and Shirley Revels for their technical assistance.

This study was supported by grants from the National Institutes of Health (HL-17670, HL-27105 and HL-07107) for M.L. and by Institutional funds of the University of Arkansas for Medical Sciences for S.L.

References

Anderson, M.P., Rich, D.P., Gregory, R.J., Smith, A.E., Welsh, M.J. 1991. Generation of cAMP-activated chloride currents by expression of CFTR. *Science* **251:**679–682

Bahinski, A., Nairn, A.C., Greengard, P., Gadsby, D.C. 1989. Chloride conductance regulated by cyclic AMP-dependent protein kinase in cardiac myocytes. *Nature* **340:**718–721

Bouron, A., Potreau, D., Raymond, G. 1991. Possible involvement of a chloride conductance in the transient outward current of whole-cell voltage-clamped ferret ventricular myocytes. *Pfluegers Arch.* **419:**534–536

Duan, D.-Y., Fermini, B., Nattel, S. 1992. Sustained outward current observed after I_{to1} inactivation in rabbit atrial myocytes is a novel Cl^- current. *Am. J. Physiol.* **263:**H1967–H1971

Hamill, O.P., Marty, A., Neher, E., Sakmann, B., Sigworth, F.J. 1981. Improved patch-clamp techniques for high-resolution current recording from cells and cell-free membrane patches. *Pfluegers Arch.* **391:**85–100

Harvey, R.D., Hume, J.R. 1989. Autonomic regulation of a chloride current in heart. *Science* **244:**983–985

Horres, C.R., Lieberman, M., Purdy, J.E. 1977. Growth orientation of heart cells on nylon monofilament. *J. Membrane Biol.* **34:**313–329

Hwang, T.-C., Horie, M., Gadsby, D.C. 1993. Functionally distinct phospho-forms underlie incremental activation of protein kinase-regulated Cl^- conductance in mammalian heart. *J. Gen. Physiol.* **101:**629–650

Liu, S., Stimers, J.R., Lieberman, M. 1992. Cyclic AMP-activated chloride current in cultured chick cardiac myocytes. *Pharmacologist* **34:**145 (*Abstr.*)

Matsuoka, S., Ehara, T., Noma, A. 1990. Chloride-sensitive nature of the adrenaline-induced current in guinea-pig cardiac myocytes. *J. Physiol.* **425:**579–598

Matsuura, H., Ehara, T. 1992. Activation of chloride current by purinergic stimulation in guinea pig heart cells. *Circ. Res.* **70:**851–855

Palade, P.T., Barchi, R.L. 1977. On the inhibition of muscle membrane chloride conductance by aromatic carboxylic acids. *J. Gen. Physiol.* **69:**879–896

Sorota, S. 1992. Swelling-induced chloride-sensitive current in canine atrial cells revealed by whole-cell patch-clamp method. *Circ. Res.* **70:**679–687

Tseng, G.-N. 1992. Cell swelling increases membrane conductance of canine cardiac cells: Evidence for a volume-sensitive Cl channel. *Am. J. Physiol.* **262:**C1056–C1068

Walsh, K.B. 1991. Activation of a heart chloride current during stimulation of protein kinase C. *Mol. Pharmacol.* **40:**342–346

Zygmunt, A.C., Gibbons, W.R. 1991. Calcium-activated chloride current in rabbit ventricular myocytes. *Circ. Res.* **68:**424–437

Zygmunt, A.C., Gibbons, W.R. 1992. Properties of the calcium-activated chloride current in heart. *J. Gen. Physiol.* **99:**391–414